Hydrothermal Crystal Growth of 2-D and 3-D Barium Rare Earth Germanates: $BaREGeO_4(OH)$ and $BaRE_{10}(GeO_4)_4O_8$ (RE=Ho,Er)

Kyle Fulle, Liurukara. D. Sanjeewa, Colin D. McMillen, Joseph W. Kolis*

Department of Chemistry and Center for Optical Materials Science and Engineering Technologies (COMSET), Clemson University, Clemson, South Carolina 29634-0973, USA

ABSTRACT

Two new structural types of $BaREGeO_4(OH)$ and $BaRE_{10}(GeO_4)_4O_8$ ($RE=Ho^{3+}$-Er^{3+}) single crystals were synthesized via high temperature and high pressure hydrothermal synthesis. The crystal structure of $BaREGeO_4(OH)$ was found to crystallize in the orthorhombic space group *Pbca* and contain a one-dimensional chain (1-D) of rare-earth polyhedra linked through edge sharing of oxygen atoms. High density $BaRE_{10}(GeO_4)_4O_8$ crystals crystallize in monoclinic space group *C2/m* and feature a sheet like arrangement of rare-earth oxide polyhedra with a Keggin-like arrangement. Barium polyhedra and isolated GeO_4 units aid in connecting the metal oxide framework to extend it in three-dimensional (3-D) space.

1. INTRODUCTION

The pursuit of new inorganic materials with the capacity to host trivalent rare-earth ions for application as phosphors and scintillators is an ongoing area of research [1]. In this context, understanding the site symmetry of host materials is critical to understanding or anticipating the luminescence spectroscopy of trivalent rare-earth ions in novel compounds. The rare earth silicates have a very rich chemistry and the discovery of new phases shows little indication of slowing down. [2][3][4][5][6][5][7][8][9] Despite the emergence of germanate crystals $Bi_4Ge_3O_{12}$ (BGO) and $BiY_{1-x}RE_xGeO_5$ ($RE=Eu^{3+}$) as potential scintillators and emitters some years ago, investigation of rare-earth (RE=La-Lu, Y) germanates has not received as much attention as rare earth

silicates.[10,11] It should be noted however that a number of interesting new alkali rare-earth germanates, including but not limited to, $NaEu_3(GeO_4)_2(OH)_2$, $NaREGeO_4$ (RE=Sm-Lu), $KLa_9(GeO_4)_6O_2$, $Na_5RE_4F(GeO_4)_4$ (RE= Pr, Nd), $Na_5Nd_4Ge_4O_{16}(OH)$, $Na_2NdGeO_4(OH)$, $K_2TbGe_2O_7$, $KEuGe_2O_6$, and $Na_3ErSi_3O_9$ have been prepared recently by solid-state and hydrothermal techniques [12–21]. In general the differences in structural chemistry between the silicates and germanates can be significant, certainly different enough to justify a detailed comparative study of their respective chemistries.[22]

The Of the reported alkaline rare-earth germanates, $Ca_2Gd_2Ge_2O_9$, $Ca_3RE_2Ge_3O_{12}$ (RE=Pr^{3+}-Gd^{3+}, Dy^{3+}), $CaEu_2Ge_3O_{10}$, $CaRE_2Ge_4O_{12}$ (RE=Eu^{3+}-Lu^{3+}), $MgLa_2GeO_6$, $Be_2RE_2GeO_7$ (RE=La^{3+}-Er^{3+}) and well-studied rare-earth oxy-apatites, no synthetic details of barium rare-earth germanate oxides or oxy-hydroxides have been reported to date [15,23–30]. The optical properties of the rare earth germanates are of particular interest. For example, the 1.54 μm luminescence of Er^{3+} ($4f^{11}$) from spin-orbit levels $^4I_{13/2}\rightarrow{}^4I_{15/2}$ is well sought for eye-safe emission [31]. Additionally, upconversion of Ho^{3+} ($4f^{10}$) in transparent glass ceramics have been linked to transitions from spin-orbit levels $^5F_5\rightarrow{}^5I_8$ which are viable alternatives for production of red emission (650 nm) in solid-state displays [32]. These optically active ions have been co-doped into bismuth germanate glasses to allow energy transfer from Er^{3+} $^4I_{13/2}$ state to Ho^{3+} $^5I_7$ state for subsequent emission of 2 μm lasing in the eye-safe region [33]. Typically these samples are prepared by conventional solid-state techniques in the form of powders. For detailed studies and optimized performance it is often desirable to prepared the materials has high quality single crystals. As such it is be desirable to undertake a systematic effort to develop a reliable route to single crystals of rare earth germanates. For the most part metal germanate single crystals have been synthesized using either a flux growth or a hydrothermal method similar to the growth of rare

earth silicates. The hydrothermal technique is a particularly attractive method for the examination of germanates because amphoteric oxides tend to grow well in the presence of basic mineralizers. We found that moderately high growth temperatures (600-700˚C) present an excellent intermediate thermal regime, which is cool enough to stabilize a wide range of phases but high enough to induce sufficient solubility for high quality crystal growth.

In this paper we describe the use of a high temperature hydrothermal growth method to prepare single crystals of the first in a series of several new rare earth germanates. We investigate holmium and erbium as the initial rare earth ions because of their interesting optical activity. The introduction of barium ions in the reaction was also included to ascertain the role of counterions in new phases. The presence of an innocent divalent ion performs several functions. It provides a divalent prototype ion that may be systematically replaced with other divalent ions of different size to expand the structural possibilities of this class of new phases. The ion can also be subsequently replaced with a more active metal such as a divalent first row transition metal with different magnetic and optical properties. Herein, we report the hydrothermal crystal growth, crystal structure and supporting characterization of two new rare earth germanate phases, $BaREGeO_4(OH)$ and $BaRE_{10}(GeO_4)_4O_8$ ($RE=Ho^{3+}$-Er^{3+}), both of which display interesting new layered structure types.

2. EXPERIMENTAL

2.1 Hydrothermal crystal growth

The title compounds $BaREGeO_4(OH)$ and $BaRE_{10}(GeO_4)_4O_8$ ($RE=Ho^{3+}$-Er^{3+}) were prepared through direct reaction of BaO, RE_2O_3 and GeO_2 powders via high temperature and high pressure

hydrothermal synthesis. As a typical example, $BaHoGeO_4(OH)$ and $BaHo_{10}(GeO_4)_4O_8$ were prepared by combining BaO (36 mg, 233 mmol; Alfa Aesar, 99.0%), Ho_2O_3 (74 mg, 195 mmol; HEFA Rare Earth, 99.99%) and GeO_2 (41 mg, 389 mmol; Alfa Aesar, 99.9%) in a 3:2.5:5 ratio, respectively. The starting materials were reacted isothermally at 650°C for 7 days in welded silver (99.9%) (1/4" x 2.5") ampoules loaded into a Tuttle cold seal autoclave constructed from Inconel 718 material. The ampoules were loaded with the appropriate component oxide feedstock and weld sealed from both ends after addition of 0.4 mL of 6 *M* CsOH as a mineralizer. Upon completion of reaction, the silver ampoules were opened and washed with DI water. In each reaction, $BaREGeO_4(OH)$, $BaRE_{10}(GeO_4)_4O_8$ and $RE_{13}Ge_6O_{31}(OH)$ crystals constituted an approximate 10/80/10 ratio of products, respectively. Single crystals of $BaREGeO_4(OH)$ and $RE_{13}Ge_6O_{31}(OH)$ were produced as polyhedral crystals approximately 0.25-0.45 mm in size and were distinguished by SCXRD unit cell determinations. $BaRE_{10}(GeO_4)_4O_8$ constituted the majority crystalline product and were identified as thick hexagonal plate crystals, with some striations in the surface, ranging from 0.15-0.35 mm in size.

2.2 X-Ray Diffraction and IR Characterization

Single crystal structure characterization was conducted using a Bruker D8 Venture single crystal diffractometer with an Incoatec Mo Kα microfocus source and Photon 100 CMOS detector. Data were collected at room temperature using phi and omega scans, and subsequently processed and scaled using the Apex3 (SAINT and SADABS) software suites [34]. Space group determinations were unambiguously made based on the systematic absences. The structures were solved by direct methods and refined to convergence by full-matrix least squares on F^2 using the SHELXTL software suite [35]. All atoms were refined anisotropically. $BaRE_{10}(GeO_4)_4O_8$

(RE=Ho, Er) was solved as a two-component twin using the program cell_now to determine the unit cell contributions and TWINABS to integrate the component reflections [36]. For $BaRE_{10}(GeO_4)_4O_8$ the major and minor component are 85.5/14.5% for Ho^{3+}, and 50.5/49.5% for Er^{3+}, respectively. Energy dispersive X-ray analysis (EDX) was used to confirm the ratio presence of Ba^{2+} over Cs^{+} in both structure types and to support the assigned ratio of metals. EDX was collected on an Oxford INCA EDX analyzer connected to a Hitachi SU6600 scanning electron microscope with a Cu standard. Powder X-ray diffraction (PXRD) was performed using a Rigaku Ultima IV diffractometer with CuK_α radiation (λ= 1.5406 Å) at 0.02° intervals at a rate of 0.25°/min from 5-65°.

The presence of hydroxide groups in BaREGeO4(OH) (RE=Ho, Er) species was confirmed from infrared spectroscopy measured by a Nicolet Magna 550 FTIR spectrometer. Data were collected from 400-4000 cm^{-1} under flowing nitrogen

2.3 Raman Single Crystal Scattering

Raman measurements were performed using an Olympus IX71 inverted microscope with a 20x objective lens coupled to a TRIAX 552 spectrometer equipped with a thermoelectrically cooled CCD detector (Andor Technology, Model DU420A-BV) operating at -60°C. An argon ion laser (Innova 100, Coherent) was used to excite the Raman signal with 514.5 nm light in a 180° backscattering geometry. A PR-550 broadband polarization rotator (Newport Corp.) was used to rotate the polarization of the incident laser source. All spectra were processed and figures prepared with Spectra-Solve for Windows software (Las Tek Pty. Ltd.) Data were collected with a laser output power of 100 to 200mW with a 2-minute integration time.

Table 1. Crystallographic data of rare earth germanates and germanate hydroxides determined by single crystal X-ray diffraction.

empirical formula	**$BaHo_{10}(GeO_4)_4O_8$**	**$BaEr_{10}(GeO_4)_4O_8$**	**$BaHoGeO_4(OH)$**	**$BaErGeO_4(OH)$**
formula weight (g/mol)	2461.00	2484.30	455.87	458.20
crystal system	monoclinic	monoclinic	orthorhombic	orthorhombic
space group, *Z*	*C2/m* (no.12), *2*	*C2/m* (no.12), *2*	*Pbca* (no.61), *8*	*Pbca* (no.61*), 8*
temperature, K	298(2)	298(2)	298(2)	298(2)
crystal size (mm)	0.08 x 0.1 x 0.1	0.07 x 0.07 x 0.07	0.02 x 0.05 x 0.07	0.08 x 0.08 x 0.09
a, Å	12.4972(5)	12.4533(8)	5.7175(2)	5.7100(2)
b, Å	7.2444(3)	7.2008(5)	10.1556(5)	10.1511(5)
c, Å	12.0170(5)	12.0034(8)	16.6189(9)	16.5766(8)
β, º	100.249(2)	100.183(2)	---	---
volume, $Å^3$	1070.60(8)	1059.43(12)	964.97(8)	960.83(7)
calculated density ($\mu g/m^3$)	7.634	7.788	6.276	6.335
absorption coefficient (mm^{-1})	43.891	46.619	30.420	31.550
F(000)	2092	2112	1568	1576
Tmax, Tmin	0.2642, 1.0000	0.2191, 1.000	0.6135, 1.000	0.5321, 1.0000
Θ range for data	3.26-30.58	3.28-28.29	4.01-26.50	4.02-26.49
reflections collected	2443	1790	7359	8926
data/restraints/parameters	2443/6/107	1790/12/107	1002/1/77	993/1/77
final R [$I > 2\sigma(I)$] R1, wR2	0.0362, 0.0785	0.0440, 0.1184	0.0213, 0.0382	0.0161, 0.0316
final R (all data) R1, wR2	0.0425, 0.0810	0.0483, 0.1216	0.0296, 0.0404	0.0195, 0.0325
goodness-of-fit on F^2	1.131	1.087	1.102	1.196
largest diff. peak/hole, e/ $Å^3$	3.831, -2.448	3.605, -2.855	0.893, -1.076	0.628, -1.073

3. RESULTS AND DISCUSSION

3.1 Crystal Structure of $BaREGeO_4(OH)$ ($RE=Ho^{3+}$-Er^{3+})

The $BaREGeO_4(OH)$ (RE=Ho^{3+}-Er^{3+}) compounds in the current study crystallize in the orthorhombic space group *Pbca* (No. 61). The two compounds are isostructural, with the Er^{3+} analog exhibiting slightly contracted cell parameters compared to Ho^{3+}. $BaHoGeO_4(OH)$ will be discussed in detail as the prototypical structure. Bond distances for $BaHoGeO_4(OH)$ and $BaErGeO_4(OH)$ are reported in Supplemental Information (**S.I.**) along with bond valance sums for metal oxide coordination. The structure is based on seven-coordinate HoO_7, BaO_{10} and isolated

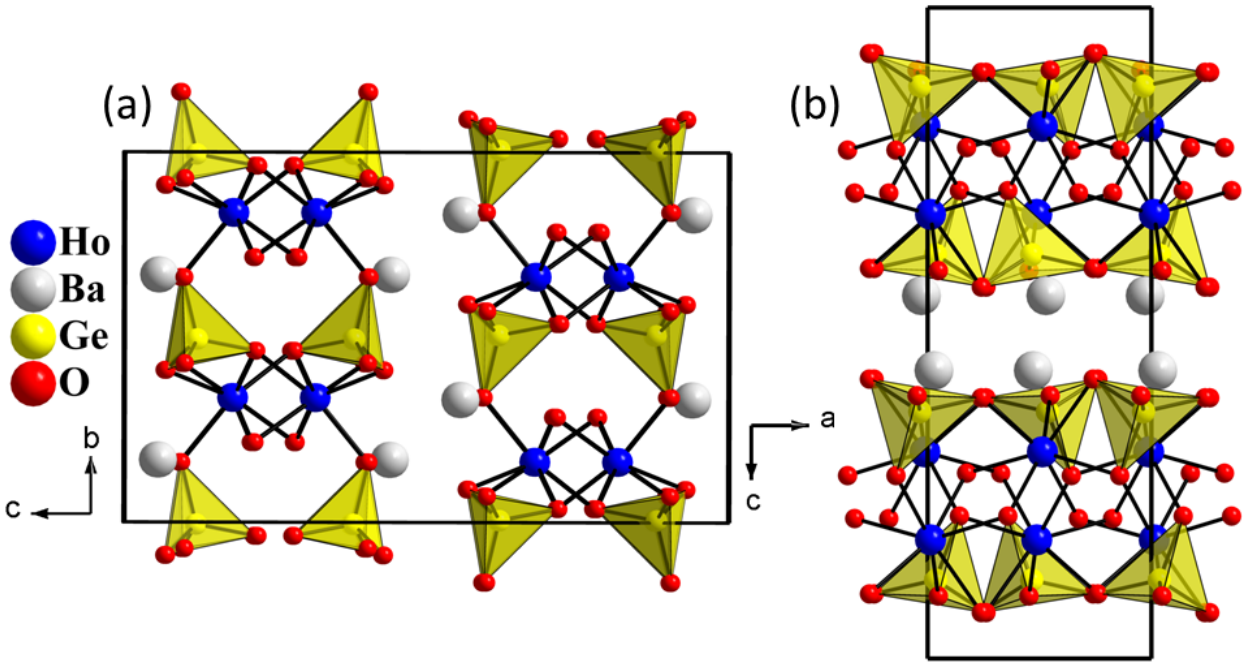

Figure 1. **a)** Isolated GeO_4 units connect holmium polyhedra in the (001) plane with barium atoms residing between layers. **b)** Holmium oxide polyhedra extending along the [100] direction through edge sharing of oxygen atoms to form a one-dimensional rare-earth oxide chain.

GeO_4 tetrahedra. All atoms reside on general crystallographic positions with *8c* Wyckoff symmetry. As seen in Fig 1, infinite zigzag chains of HoO_7 polyhedra run parallel to the *a*-axis via edge sharing of O(4) and O(5) atoms and are the key structural component to the framework. Isolated GeO_4 units interconnect these HoO_7 chains along the *ab*-plane via corner-sharing of O(1) and O(3), and edge-sharing of O(2) and O(4) oxygen atoms.

Each GeO_4 unit coordinates four holmium atoms and connects two isolated HoO_7 chains. This framework forms alternating layers of HoO_7 polyhedra and GeO_4 units. Additionally, GeO_4 units orient relative to the *b*-axis in an alternating fashion as is visible in **Fig(1a)**. Thus, this layered framework is built up by the corner and edge-shared HoO_7 and GeO_4 polyhedra, between which the barium atoms reside to maintain charge balances. The HoO_7 polyhedra form distorted trigonal prismatic, square face monocapped geometry with Ho-O bond distances ranging from 2.262(4)-2.433(4) Å with an average of 2.33 Å. GeO_4 tetrahedra exhibit bond distances ranging from 1.742(4)-1.771(4) Å with an average distance of 1.75 Å. The existence of barium atoms in the framework creates an intricate three-dimensional network. The barium atoms exist as irregular polyhedra with Ba-O distances between 2.579(4)-3.241(4) Å and averaging 2.94 Å. Bond valance sum calculations resulted in values of 1.94, 3.10, and 3.93 for Ba^{2+}, Ho^{3+}, and Ge^{+4}, respectively, consistent with the assigned oxidation states [37,38]. Oxygen atom O(5) is suspected as the hydroxide by bond valance sum considerations and O(5) being the only non-bonding germanium oxygen. Bond valence sum of the O(5) atom is 1.15, and other oxygen atoms exhibit values of 1.79-2.11, supporting the assignment of OH^- and O^{2-}, respectively. The hydroxide group points generally toward the vacancy formed between germanate and holmium polyhedra. The presence of hydroxide is supported by IR of $BaHoGeO_4(OH)$ and $BaErGeO_4(OH)$ with single crystal Raman indicating a strong stretching mode at 3420 cm^{-1} for $BaHoGeO_4(OH)$, (**S.I**.). Semiquantitative elemental analysis (EDX) was used to support the 1:1:1 ratio of metals and supports the assignment of Ba^{2+} over Cs^+ in the framework, with no evidence of a mixed metal site (**S.I**.).

The formula of this new barium rare-earth oxy-hydroxides discussed herein are somewhat reminiscent of the sodium rare-earth germanate species $Na_2NdGeO_4(OH)$, synthesized by mild hydro-flux of sodium hydroxide [17]. Both structures exhibit one-dimensional zigzag chains of

rare-earth polyhedra. However, these structures are not isostructural as $Na_2NdGeO_4(OH)$ chains interconnect via corner sharing of O(4) atoms forming an intricate rare-earth framework, while $BaREGeO_4(OH)$ exhibits truly isolated one-dimensional chains interconnected through isolated GeO_4 building blocks.

3.2 Crystal Structure of $BaRE_{10}(GeO_4)_4O_8$ ($RE=Ho^{3+}$-Er^{3+})

The crystal structure of $BaRE_{10}(GeO_4)_4O_8$ ($RE=Ho^{3+}$-Er^{3+}) represents a new barium rare earth germanate with BaO_8, HoO_6, HoO_7 and GeO_4 building blocks. The structures are isostructural with the Er^{3+} unit cell parameters being slightly constricted as expected.

Figure 2. $BaHo_{10}(GeO_4)_4O_8$ view along the [010] projection. **(a)** Sheet-like arrangement of

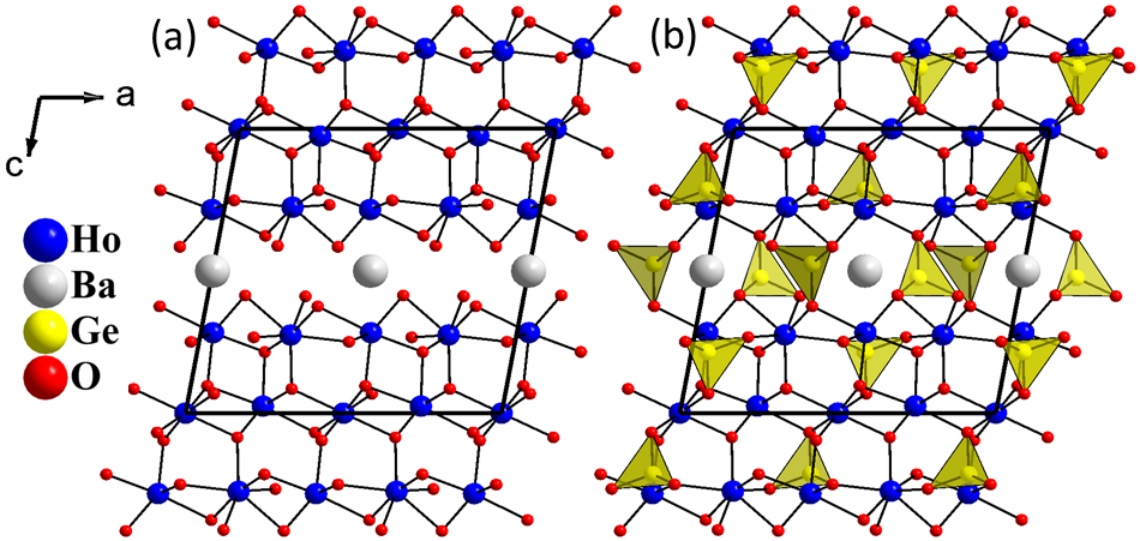

holmium oxide polyhedra extending in the *ab*-plane with Ba^{2+} ions occupying void between layers. (**b**) Isolated GeO_4 units stabilize the rare-earth framework and encapsulate the Ba^{2+} ions in channels along [010] direction.

Again the holmium analog, $BaHo_{10}(GeO_4)_4O_8$, will be discussed in detail as the prototypical structure. The structure type contains four unique crystallographic Ho^{3+} sites: $Ho(1)O_7$ (*4i*), $Ho(2)O_7$ (*4i*), $Ho(3)O_7$ (*8j*), and $Ho(4)O_6$ (*4g*) with Ho(1)/Ho(2) residing on mirror planes and

Ho(4) inhabiting a 2-fold symmetry site. The Ho-O bond distances range from 2.187(5)-2.490(7) Å for the four holmium polyhedra. The compound forms a complex framework of HoO_6 and HoO_7 polyhedra that form sheets propagating along the *ab*-plane.

Within the rare-earth oxide framework, two distinct connectivities are observed. The first framework is built up of Ho(4) polyhedra that interconnect through edge sharing of O(4) and O(9) atoms in the *ab*-plane. These chains interconnect through Ho(2) polyhedra coordinating through μ_3 bridging of O(2), O(4) and O(9) to construct a honeycomb-type lattice (**Fig. 3a**).

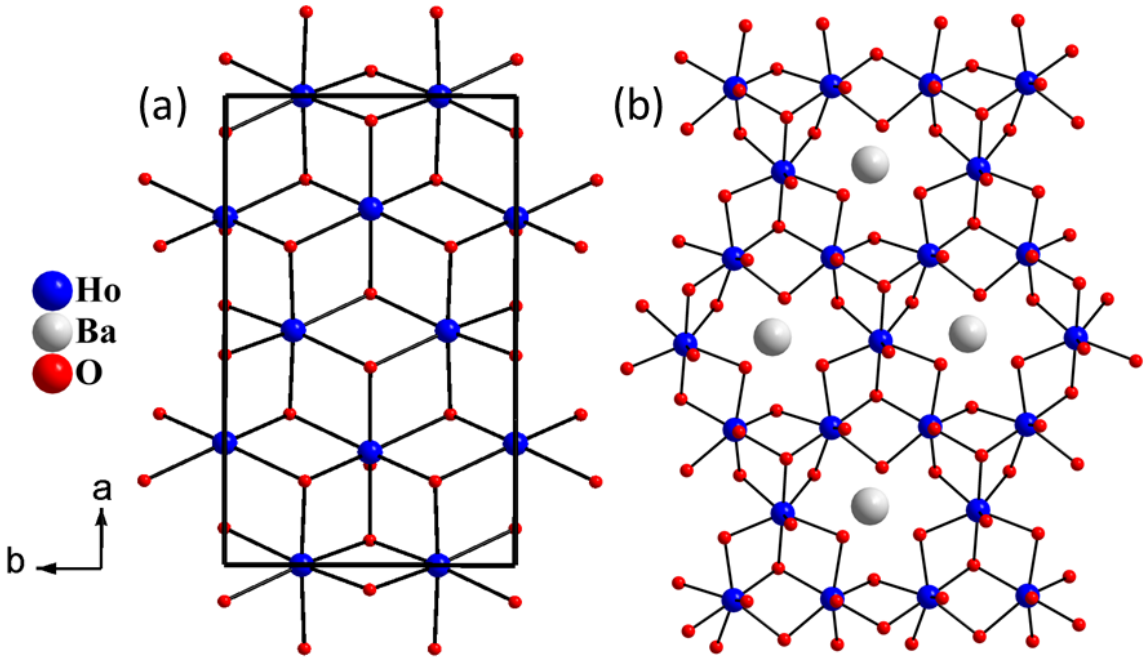

Figure 3. **(a)** Ho(2) and Ho(4) polyhedra forming a honeycomb-type of arrangement visible along the [001] direction. **(b)** Ho(1) and Ho(3) polyhedra creating distorted channels with Ba^{2+} ions coordinating the center to provide additional structural support and charge balance.

of O(1), O(3), O(7) and O(8) with μ_3 bridging of O(5) and O(6). This connectivity forms Simultaneously, the Ho(1) and Ho(3) polyhedra form a planar network constructed from edge sharing distorted channels along the *c*-axis in which barium atoms can be observed (**Fig. 3b**). The Ho(1) and Ho(3) polyhedra form a cap with the Ho(2)/Ho(4) honeycomb lattice residing within this cap and interconnecting through μ_4 bridging of O(2) and O(4) This framework of Ho^{3+}

polyhedra forms a sheet which propagates in the *ab*-plane with barium atoms separating the layers (**Fig. 2a**) and providing the necessary charge balance.

Isolated GeO_4 tetrahdera support the solid-state framework, (**Fig 2b).** Two crystallographically distinct germanium sites, Ge(1) and Ge(2), reside on *4i* Wyckoff sites with mirror symmetry. Ge-O bond distances range from 1.734(9)-1.748(9) Å for the two germanium sites. Ge(1) coordinates nine holmium polyhedra and resides within the holmium oxide framework. Ge(1) coordinates a trimeric unit of Ho(2) and Ho(4) x2 through μ_4 bridging of O(9) above the tetrahedral site in the *ab*-plane. Simultaneously, Ge(1) coordinates two six holmium centers through corner-shared O(1) and O(3) x2. The Ge(1) tetrahedra link the rare-earth sheet framework while $Ge(2)O_4$ tetrahedra create the void between layers by coordinating to barium atoms. These same tetrahedra also coordinate to six holmium atoms and reside between the rare-earth sheets with neighboring barium atoms, thus strengthening the layered structure. Ho(1) and Ho(3)(x2) form a trimeric unit that connect through μ_4 bridging of O(6) above the tetrahedral site and below through edge sharing of O(7) and O(8) atoms. Ge(2) alternates up/down direction relative to the *c*-axis while propagating along the *ab*-plane (**Fig.2b**). Bond valence sum calculations resulted in values of 1.72, 3.06, 2.99, 2.94, 2.95, 4.08, 4.03 for Ba(1), Ho(1), Ho(2), Ho(3), Ho(4), Ge(1) and Ge(2), respectively, consistent with the assigned oxidation states. The absence of hydroxide is supported by IR as well as single crystal Raman which indicate no observation of potential OH^- stretches in the region from 3600-3200 cm^{-1} in $BaHo_{10}(GeO_4)_4O_8$, (**S.I**.). Semiquantitative elemental analysis (EDX) was used to support the ratio of metals and supports the assignment of Ba^{2+} in the framework, with no evidence of Cs+ ions in the structure (**S.I**.).

3.3 Single Crystal Raman Characterization

Both $BaHoGeO_4(OH)$ and $BaHo_{10}(GeO_4)_4O_8$ where investigated by single crystal Raman scattering as representatives of each new structural type to determine fundamental stretching and bending modes for the isolated GeO_4 units. For each GeO_4^{3-} anion, nine internal Raman vibrational modes are expected from the general formula $3n$-6. The GeO_4^{3-} anions in the reported germanates adopt T_d point group symmetry, and their internal vibrations can be described by A_1 and E Raman active modes, and $2T_2$ Raman and IR active modes. Both structures show strong bands from 700-825 cm^{-1}, which have been assigned as symmetric υ_1 and asymmetric υ_3 stretching modes for the GeO_4 building block. $BaHo_{10}(GeO_4)_4O_8$ shows two peaks at which correspond to the υ_4 bending internal modes of the GeO4 tetrahedra. This is commensurate with known rare-earth apatite $La_{8+x}Ba_{2-x}(GeO_4)_6O_{2+x/2}$ (x= 0 and 1.2) structural types in which the scattering bands at similar wavenumbers were assigned these corresponding modes isolated GeO_4 units [39].

4. Summary and Conclusions

While the rare earths have often been viewed as a monotonic chemical block, their structural chemistry in the presence of oxyanion building blocks such as silicates indicates that this is not true. [40][2] In particular the chemistry across the f-block ion silicates in hydrothermal aqueous fluids has consistently shown an unexpectedly diverse behavior, leading to the emergence of a wide range new materials with interesting solid-state frameworks. Recently, we investigated the chemistry of barium rare-earth silicates ($Ba_2RE_2Si_4O_{13}$) (RE= La^{3+}-Ho^{3+}) and barium rare-earth silicate fluorides ($Ba_2RE_2Si_4O_{12}F_2$) (RE=Er^{3+}-Lu^{3+}) in high temperature and high-pressure hydrothermal conditions to determine the effect of rare-earth size on phase transitions between these structures. [40] In a the logical extension of this work we began investigation the chemistry

of rare earth germanates in hydrothermal fluids, typically using aqueous bases such CsOH as a mineralizer. The tetrahedral building blocks of silica and germanium oxide also show very different structural chemistry despite belonging to the same periodic group and displaying similar coordination chemistry. The structural chemistry of metal germanates is further complicated by the fact that, unlike silicates, germanates often display coordination environments other than tetrahedral (five- and six-coordinate), which makes the possible phase space even greater. [41]

Interestingly, although the polygermanates show a very rich structural chemistry in Ge-O frameworks, there are fewer examples of germanates directly coordinated to rare earth metal centers where the germanates are not just tetrahedra or polymeric tetrahedra like the silicates. There are a number of interesting uranium compounds with unusual polygermanate building blocks beyond the conventional tetrahedra that were synthesized using high temperature hydrothermal methods.[42][43] These interesting compounds strongly suggest that rare earth germanates with non-tetrahedral building blocks can be synthesized and isolated under appropriate hydrothermal conditions. We began a systematic examination of the phase space of rare earth germanates under these typical high temperature hydrothermal reaction conditions with the belief that a menu of isolated tetrahedral germanates, various polymeric germanate clusters and of non-tetrahedral germanate building blocks, along with a wide variety of coordination environments of the rare earth ions, would combine to provide an almost infinite possibility of new structure types. Our long term goal is to be able to provide some degree of predictability to this chemistry in order to extract the maximum degree of performance of luminescent, lasing, magnetic and other useful properties of the germanates. We feel that a high temperature hydrothermal approach is an attractive one because of the chemical flexibility that it provides as well as its ability to form high

quality crystals of materials whose parent oxie building blocks are extremely refractory in nature. [44]. As we expected the approach does lead to a wide range on new materials and these are currently under investigation. [45] In this paper we describe out initial results using two rare earth (Er, Ho) ions in the middle of the f-block that typically display interesting spectroscopic properties which leads to two interesting new structural types.

The reaction of barium oxide, select rare-earth oxides, and germanium oxide in hydrothermal fluids was done using a hydroxide mineralizer of 6 *M* CsOH. Two new stable products were isolated. $BaREGeO_4(OH)$ (RE=Ho, Er) single crystals formed as a minor hydrothermal product as good single crystals (0.25 mm). This new structure type displays an isolated one-dimensional chain of rare-earth polyhedra that are connected through edge sharing of oxygen atoms of isolated GeO_4 building blocks forming sheets with Ba^{2+} ions between layers. A second product major product $BaRE_{10}(GeO_4)_4O_8$ (RE=Ho, Er) displays a unique sheet-like arrangement involving four unique rare-earth sites separated by Ba^{2+} ions and coordinated by isolated GeO_4 units.

Compared to recently investigated rare earth silicates, the phase stability of the barium rare-earth germanates appears much more complex. While the SiO_4 and GeO_4 building blocks display many of the same coordination features, the hydrothermal chemistry of these rare-earth building blocks are thus far quite different. The IR, Raman and photoluminescence spectroscopy also correlated well with the observes structures The introduction of barium ions in the chemistry provides an additional chemical and structural variability. To our knowledge this is the first example of a rare earth germanate containing a barium ion. These preliminary results suggest that a wide range of

new rare earth germanates will isolated as large single crystals and their magnetic and optical properties can be studied.

ACKNOWLEDGMENT

The authors thank the Department of Energy Basic Energy Sciences DE-SC0014271for financial support.

References:

Zotero updates this list each time changes are made to citations. Best to add subscripts/superscripts last.

[1] M.S. Wickleder, Inorganic Lanthanide Compounds with Complex Anions, Chem. Rev. 102 (2002) 2011–2088. doi:10.1021/cr010308o.

[2] M. Wierzbicka-Wieczorek, U. Kolitsch, E. Tillmanns, Synthesis and structural study of five new trisilicates, $BaREE_2Si_3O_{10}$ (REE = Gd, Er, Yb, Sc) and $SrY_2Si_3O_{10}$, including a review on the geometry of the Si_3O_{10} unit, Eur. J. Mineral. 22 (2010) 245–258. doi:10.1127/0935-1221/2010/0022-1969.

[3] J. Felsche, The crystal chemistry of the rare-earth silicates, in: Rare Earths, Springer, Berlin, Heidelberg, 1973: pp. 99–197. doi:10.1007/3-540-06125-8_3.

[4] M. Wierzbicka-Wieczorek, U. Kolitsch, E. Tillmanns, Ba2Gd2(Si4O13): a silicate with finite Si4O13 chains, Acta Crystallogr. C. 66 (2010) i29–i32. doi:10.1107/S0108270110002842.

[5] I. Vidican, M.D. Smith, H.-C. zur Loye, Crystal growth, structure determination, and optical properties of new potassium-rare-earth silicates K3RESi2O7 (RE=Gd, Tb, Dy, Ho, Er, Tm, Yb, Lu), J. Solid State Chem. 170 (2003) 203–210. doi:10.1016/S0022-4596(02)00029-4.

[6] S.M. Haile, B.J. Wuensch, X-ray diffraction study of K3NdSi7O17: a new framework silicate with a linear Si—O—Si bond, Acta Crystallogr. B. 56 (2000) 773–779. doi:10.1107/S0108768100006704.

[7] M. Wierzbicka-Wieczorek, U. Kolitsch, E. Tillmanns, The Crystal Structures of Three New Complex Silicates of Scandium, Can. Mineral. 48 (2010) 51–68. doi:10.3749/canmin.48.1.51.

[8] M. Wierzbicka-Wieczorek, P.K. Krug, U. Kolitsch, High-Temperature Flux Growth as a Tool for the Preparation of Mixed-Framework Metal-Y Silicates: A Systematic Evaluation of the Influence of Experimental Parameters, Cryst. Growth Des. 17 (2017) 590–603. doi:10.1021/acs.cgd.6b01448.

[9] S.M. Haile, B.J. Wuensch, T. Siegrist, R.A. Laudise, Conductivity and crystallography of new alkali rare-earth silicates synthesized as possible fast-ion conductors, Solid State Ion. 53 (1992) 1292–1301. doi:10.1016/0167-2738(92)90328-M.

[10] C. Cascales, C. Zaldo, Crystal-field analysis of Eu3+ energy levels in the new rare-earth R BiY1−xRxGeO5 oxide, J. Solid State Chem. 171 (2003) 262–267. doi:10.1016/S0022-4596(02)00173-1.
[11] M. Goyot, B. Ille, P. Lebrun, J.P. Martin, Performances of a preamplifier-silicon photodiode readout system associated with large BGO crystal scintillators, Nucl. Instrum. Methods Phys. Res. Sect. Accel. Spectrometers Detect. Assoc. Equip. 263 (1988) 180–187. doi:10.1016/0168-9002(88)91032-7.
[12] X. Zhao, T. Yan, K. Wang, Y. Yan, B. Zou, J. Yu, R. Xu, NaEu3(GeO4)2(OH)2: A High-Pressure-Stable Photoluminescent Lanthanide Germanate, Eur. J. Inorg. Chem. 2012 (2012) 2527–2532. doi:10.1002/ejic.201200200.
[13] M. Emirdag-Eanes, M. Krawiec, J.W. Kolis, Hydrothermal synthesis and structural characterization of NaLnGeO4 (Ln = Ho, Er, Tb, Tm, Yb, Lu) family of lanthanide germanates, J. Chem. Crystallogr. 31 (2001) 281–285. doi:10.1023/A:1014378729117.
[14] J. Yeon, J.B. Hardaway, A.S. Sefat, A.M. Latshaw, H.-C. zur Loye, Crystal growth, structures, magnetic and photoluminescent properties of NaLnGeO4 (Ln = Sm, Eu, Gd, Tb), Solid State Sci. 34 (2014) 24–30. doi:10.1016/j.solidstatesciences.2014.05.002.
[15] O.A. Lipina, L.L. Surat, A.P. Tyutyunnik, A.N. Enyashin, A.Y. Chufarov, V.G. Zubkov, Structure and optical properties of KLa9(GeO4)6O2 and KLa8.37Eu0.63(GeO4)6O2, Chem. Phys. Lett. 667 (2017) 9–14. doi:10.1016/j.cplett.2016.11.021.
[16] A.M. Latshaw, B.O. Wilkins, G. Morrison, M.D. Smith, H.-C. zur Loye, A5RE4X[TO4]4 crystal growth: Fluoride flux synthesis of Na5Ln4F[GeO4]4 (Ln=Pr, Nd), the first quaternary germanate oxyfluorides, J. Solid State Chem. 239 (2016) 200–203. doi:10.1016/j.jssc.2016.04.038.
[17] K. Hughey, J. Yeon, H.-C. zur Loye, Crystal Growth and Structure Determination of the New Neodymium Germanate, Na2NdGeO4(OH), J. Chem. Crystallogr. 44 (2014) 320–323. doi:10.1007/s10870-014-0517-3.
[18] K. Hughey, J. Yeon, H.-C. zur Loye, Crystal Growth and Structure Determination of the New Neodymium Germanate, Na5Nd4Ge4O16(OH), J. Chem. Crystallogr. 44 (2014) 376–379. doi:10.1007/s10870-014-0525-3.
[19] K. Fulle, L.D. Sanjeewa, C.D. McMillen, Y. Wen, A.C. Rajamanthrilage, J.N. Anker, G. Chumanov, J.W. Kolis, One-Pot Hydrothermal Synthesis of TbIII13(GeO4)6O7(OH) and K2TbIVGe2O7: Preparation of a Stable Terbium(4+) Complex, Inorg. Chem. 56 (2017) 6044–6047. doi:10.1021/acs.inorgchem.7b00821.
[20] P.-L. Chen, P.-Y. Chiang, H.-C. Yeh, B.-C. Chang, K.-H. Lii, Synthesis, crystal structure, magnetic and luminescence properties of KEuGe 2 O 6 : a europium cyclogermanate containing infinite chains of edge-sharing Eu–O polyhedra, Dalton Trans. 0 (2008) 1721–1726. doi:10.1039/B716654K.
[21] D. Ananias, J.P. Rainho, A. Ferreira, M. Lopes, C.M. Morais, J. Rocha, L.D. Carlos, Synthesis and Characterization of Er(III) and Y(III) Sodium Silicates: Na3ErSi3O9, a New Infrared Emitter, Chem. Mater. 14 (2002) 1767–1772. doi:10.1021/cm011550e.
[22] U.W. Becker, J. Felsche, Phases and structural relations of the rare earth germanates RE2Ge2O7, RE ≡ La-Lu, J. Common Met. 128 (1987) 269–280. doi:10.1016/0022-5088(87)90215-3.
[23] F. Piccinelli, M. Pedroni, S. Cagliero, A. Speghini, M. Bettinelli, Structural study of Ca2Gd2Ge2O9 and optical spectroscopy of the Eu3+ dopant ion, J. Solid State Chem. 212 (2014) 180–184. doi:10.1016/j.jssc.2014.01.025.
[24] F. Piccinelli, A. Lausi, M. Bettinelli, Structural investigation of the new Ca3Ln2Ge3O12 (Ln=Pr, Nd, Sm, Gd and Dy) compounds and luminescence spectroscopy of Ca3Gd2Ge3O12 doped with the Eu3+ ion, J. Solid State Chem. 205 (2013) 190–196. doi:10.1016/j.jssc.2013.07.021.

[25] O.A. Lipina, L.L. Surat, M.A. Melkozerova, A.P. Tyutyunnik, I.I. Leonidov, V.G. Zubkov, Synthesis, crystal structure and luminescence properties of CaY2−xEuxGe3O10 (x=0–2), J. Solid State Chem. 206 (2013) 117–121. doi:10.1016/j.jssc.2013.08.002.
[26] V.G. Zubkov, N.V. Tarakina, I.I. Leonidov, A.P. Tyutyunnik, L.L. Surat, M.A. Melkozerova, E.V. Zabolotskaya, D.G. Kellerman, Synthesis and crystal structure of Ln2M2+Ge4O12, Ln=rare-earth element or Y; M=Ca, Mn, Zn, J. Solid State Chem. 183 (2010) 1186–1193. doi:10.1016/j.jssc.2010.03.027.
[27] M. Swaffer, P.R. Slater, R.K. Gover, T. Matsumura, R. Kanno, T. Kamiyama, La2MgGeO6: A Novel Ge Based Perovskite Synthesized under Ambient Pressure., ChemInform. 33 (2002) 17–17.
[28] Y. Ochi, H. Morikawa, F. Marumo, H. Nozaki, Structures and magnetic properties of rare earth compounds in the melilite group, Yogyo-Kyokai-Shi. 91 (1983) 229–235.
[29] P. Berastegui, S. Hull, F.J. Garcı Garcı, J. Grins, A Structural Investigation of La2(GeO4)O and Alkaline-Earth-Doped La9.33(GeO4)6O2, J. Solid State Chem. 168 (2002) 294–305. doi:10.1006/jssc.2002.9724.
[30] A.M. Latshaw, K.D. Hughey, M.D. Smith, J. Yeon, H.-C. zur Loye, Photoluminescent and Magnetic Properties of Lanthanide Containing Apatites: NaxLn10–x(SiO4)6O2–yFy, CaxLn10–x(SiO4)6O2–yFy (Ln = Eu, Gd, and Sm), Gd9.34(SiO4)6O2, and K1.32Pr8.68(SiO4)6O1.36F0.64, Inorg. Chem. 54 (2015) 876–884. doi:10.1021/ic502185b.
[31] L.A. Bueno, A.S. Gouveia-Neto, E.B. da Costa, Y. Messaddeq, S.J.L. Ribeiro, Structural and spectroscopic study of oxyfluoride glasses and glass-ceramics using europium ion as a structural probe, J. Phys. Condens. Matter. 20 (2008) 145201. doi:10.1088/0953-8984/20/14/145201.
[32] A.S. Gouveia-Neto, E.B. da Costa, L.A. Bueno, S.J.L. Ribeiro, Intense red upconversion emission in infrared excited holmium-doped PbGeO3–PbF2–CdF2 transparent glass ceramic, J. Lumin. 110 (2004) 79–84. doi:10.1016/j.jlumin.2004.04.005.
[33] T. Ragin, M. Kochanowicz, J. Żmojda, D. Dorosz, Spectroscopic properties of bismuth-germanate glasses co-doped with erbium and holmium ions, in: 2014: p. 92280C–92280C–8. doi:10.1117/12.2067063.
[34] Apex3; Bruker AXS Inc.: Madison, WI, 2015., (n.d.).
[35] G.M. Sheldrick, Crystal structure refinement with SHELXL, Acta Crystallogr. Sect. C Struct. Chem. 71 (2015) 3–8. doi:10.1107/S2053229614024218.
[36] G.M. Sheldrick, Cell_Now and TWINABS, University of Göttingen, Germany, 2008.
[37] N.E. Brese, M. O'Keeffe, Bond-valence parameters for solids, Acta Crystallogr. B. 47 (1991) 192–197. doi:10.1107/S0108768190011041.
[38] I.D. Brown, D. Altermatt, Bond-valence parameters obtained from a systematic analysis of the Inorganic Crystal Structure Database, Acta Crystallogr. B. 41 (1985) 244–247. doi:10.1107/S0108768185002063.
[39] A. Orera, M. L. Sanjuán, E. Kendrick, V. M. Orera, P. R. Slater, Raman spectroscopy studies of apatite -type germanate oxide ion conductors: correlation with interstitial oxide ion location and conduction, J. Mater. Chem. 20 (2010) 2170–2175. doi:10.1039/B922834A.
[40] K. Fulle, L.D. Sanjeewa, C.D. McMillen, J.W. Kolis, K. Fulle, L.D. Sanjeewa, C.D. McMillen, J.W Kolis "Crystal Chemistry of the Discrete Tetrasilicate Units with Rare Earth Dimers: Ba2RE2Si4O12F2 (RE = Er-Lu) and Ba2Re2SiO13 (RE = Pr-Sm) Acta Crystallographica B 2017 in press., Acta Crystallogr. B. (2017).
[41] X. Ren, Q. Pan, J. Liu, Y. Li, F. Wang, J. Li, Y. Xu, L. Li, A family of germanates constructed from Ge7 clusters co-templated by metal complexes and organic/inorganic species, CrystEngComm. 16 (2014) 9545–9554. doi:10.1039/C4CE00671B.
[42] Q.B. Nguyen, K.-H. Lii, Cs4UGe8O20: A Tetravalent Uranium Germanate Containing Four- and Five-Coordinate Germanium, Inorg. Chem. 50 (2011) 9936–9938. doi:10.1021/ic201789f.

[43] Q.B. Nguyen, C.-L. Chen, Y.-W. Chiang, K.-H. Lii, Cs3UGe7O18: A Pentavalent Uranium Germanate Containing Four- and Six-Coordinate Germanium, Inorg. Chem. 51 (2012) 3879–3882. doi:10.1021/ic3000872.
[44] G. Adachi, N. Imanaka, The Binary Rare Earth Oxides, Chem. Rev. 98 (1998) 1479–1514. doi:10.1021/cr940055h.
[45] L.D. Sanjeewa, K. Fulle, C.D. McMillen, J.W. Kolis, Hydrothermal Chemistry of Rare Earth Germanates, Manuscr. Prep. (n.d.).
[46] M. Wierzbicka-Wieczorek, U. Kolitsch, E. Tillmanns, Ba2Gd2(Si4O13): a silicate with finite Si4O13 chains, Acta Crystallogr. C. 66 (2010) i29–i32. doi:10.1107/S0108270110002842.